Using $e^+e^- \to \nu\overline{\nu}t\overline{t}$ to Probe Strong Electroweak Symmetry Breaking at the NLC*

Timothy L. Barklow
Stanford Linear Accelerator Center, Stanford University Stanford, California 94309, USA

ABSTRACT

The potential of the reaction $e^+e^- \to \nu\overline{\nu}t\overline{t}$ for the study of strong electroweak symmetry breaking is reviewed.

I. INTRODUCTION

Processes with W and Z bosons in the final state have received most of the attention in studies of strongly interacting Higgs sectors at future colliders. Such studies have shown that the LHC and an e^+e^- linear collider with a center of mass energy of 1000–1500 GeV (the NLC) have comparable sensitivities to a strongly interacting Higgs sector. In this paper we take a different tact and study the reaction $e^+e^- \to \nu\overline{\nu}t\overline{t}$. The LHC cannot take advantage of $W^+W^- \to t\overline{t}$ because of the large background from $gg \to t\overline{t}$.

We begin by examining what would happen to Standard Model phenomenology if there were no light Higgs boson resonance.

II. THE STANDARD MODEL WITHOUT A LIGHT HIGGS BOSON

We review two processes: $f\overline{f} \to W^+W^-$ and $W^+W^- \to W^+W^-$.

A. The Reaction $f\overline{f} \to W^+W^-$

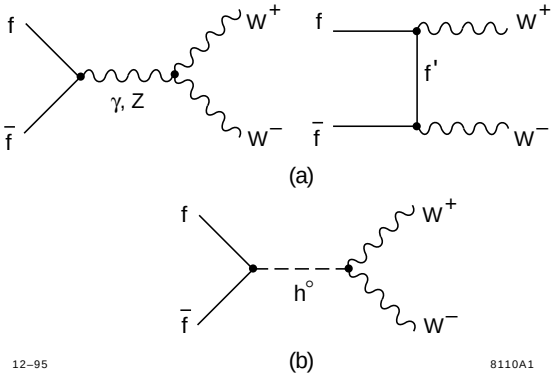

Figure 1: Standard Model Feynman diagrams for $f\overline{f} \to W^+W^-$: (a) all diagrams except for s-channel Higgs boson exchange; (b) the s-channel Higgs boson exchange diagram.

The Standard Model amplitudes for $f\overline{f} \to W^+W^-$ are displayed in Fig. 1. If the amplitudes for $f\overline{f} \to W^+W^-$ were limited to those shown in Fig. 1a, then the total amplitude would be proportional to $m_f\sqrt{s}$, where m_f is the mass of the fermion and $\sqrt{s}$ is the $f\overline{f}$ center of mass energy. For a sufficiently large center of mass energy the total amplitude would violate unitarity. This problematic high energy behavior is due to the helicity combinations $f_L\overline{f}_L \to W_L^+W_L^-$ and $f_R\overline{f}_R \to W_L^+W_L^-$, where f_L and f_R denote left and right–handed fermions, respectively, and W_L denotes a longitudinally polarized W boson. In the Standard Model the s–channel Higgs exchange amplitude of Fig. 1b is proportional to -$m_f\sqrt{s}$ and therefore cancels the contribution from the graphs of Fig. 1a, as long as the Higgs boson mass is not too large.

For $e^+e^- \to W^+W^-$, a collider with an e^+e^- center of mass energy of at least 500 TeV would be required to detect the presence or absence of a light Higgs boson from this effect. However, for $t\overline{t} \to W^+W^-$ (or $W^+W^- \to t\overline{t}$) the necessary center of mass energy is much less, due to the large top quark mass.

B. The Reaction $W^+W^- \to W^+W^-$

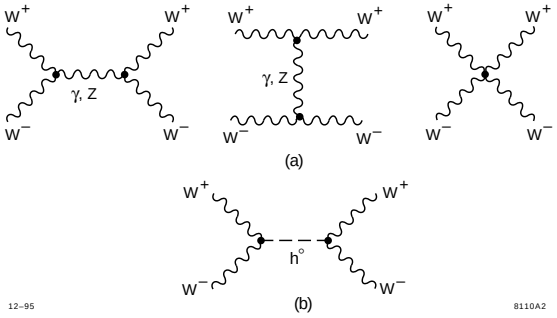

Figure 2: Standard Model Feynman diagrams for $W^+W^- \to W^+W^-$. All diagrams except for s-channel Higgs boson exchange are shown in (a). The s-channel Higgs boson exchange diagram is shown in (b).

The Standard Model amplitudes for $W^+W^- \to W^+W^-$ are displayed in Fig. 2. If the amplitudes for $W^+W^- \to W^+W^-$ were limited to those shown in Fig. 2a, then the total amplitude would be proportional to s. In the Standard Model the s–channel Higgs exchange amplitude of Fig. 2b is proportional to -s and therefore cancels the contribution from the graphs of Fig. 2a. The total amplitude is then proportional to m_H^2, where m_H is the Higgs mass. Unitarity is not violated so long as the Higgs boson mass is not too large.

Because the sum of the amplitudes in Fig. 2a diverges as s it is customarily assumed that the first indication of the absence

* Work supported by Department of Energy contract DE–AC03–76SF00515.

of a light Higgs boson would appear in $W^+W^- \to W^+W^-$ or in $W^+W^- \to ZZ$ (or in a crossed reaction). Considerable attention has therefore been paid to these reactions in studies of the physics of future colliders.

III. THE REACTION $e^+e^- \to \nu\overline{\nu}W^+W^-,\ \nu\overline{\nu}ZZ$

The analysis by Barger *et al.* [1] of the the gauge boson scattering processes $W_{\rm L}^+W_{\rm L}^- \to W_{\rm L}^+W_{\rm L}^-$ and $W_{\rm L}^+W_{\rm L}^- \to Z_LZ_L$ will serve as a model for our analysis of $W_{\rm L}^+W_{\rm L}^- \to t\bar{t}$.

Barger *et al.* use several models to test the effectiveness of their analysis:

1. Standard Model Higgs Boson with Mass $m_H = 1$ TeV.
2. Chirally–Coupled Scalar (CCS) Model (Techni–σ). A scalar mass and width of 1 TeV and 0.35 GeV, respectively, are used.
3. Chirally–Coupled Vector (CCV) Model (Techni–ρ). A technirho mass and width of 1 TeV and 0.03 TeV, respectively, are used.
4. Low–Energy Theorem (LET) Model.

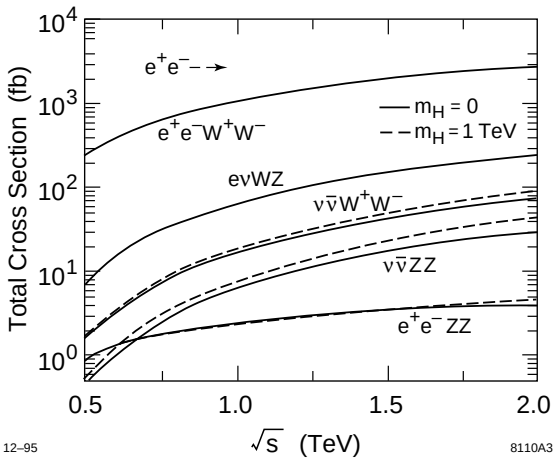

Figure 3: Total cross section versus e^+e^- center of mass energy for processes of the form $e^+e^- \to l_1\bar{l}_2V_1V_2$ where l_i denotes an electron or electron-neutrino and V_i denotes a $W^\pm$ or Z gauge boson.

The total cross section for processes of the form $e^+e^- \to l_1\bar{l}_2V_1V_2$, where l_i denotes an electron or electron-neutrino and V_i denotes a $W^\pm$ or Z gauge boson, is shown in Fig. 3 as a function of e^+e^- center of mass energy. The cross sections for the Standard Model Higgs with $m_H = 1$ TeV are given by the dashed curves and are representative of the cross sections for the strongly interacting models we have been discussing. The signal is the difference between the dashed and solid curves.

Barger *et al.* utilize a series of cuts to produce an event sample that is rich in the final states $\nu\overline{\nu}W_{\rm L}^+W_{\rm L}^-$ and $\nu\overline{\nu}Z_LZ_L$. They use the gauge boson decays $W^\pm \to j_1j_2$ and $Z \to j_1j_2$. A fairly conservative jet energy resolution of $\Delta E_j/E_j = 50\%/\sqrt{E_j} \oplus 2\%$ is assumed which results in a WW/ZZ misidentification probability of a few percent and WW/WZ, ZZ/WZ misidentification probabilities of roughly 20%. These misidentification probabilities are included in their analysis.

Events of the type $e^+e^- \to W^+W^-$ are removed with the cut

$$M_{\rm recoil} > 200\ {\rm GeV} \tag{1}$$

where $M_{\rm recoil}$ is the missing mass defined by

$$M_{\rm recoil}^2 = s + M_{WW}^2 - 2\sqrt{s}(E_{W^+} + E_{W^-})\ . \tag{2}$$

Here M_{WW} is the mass of the W^+W^- system and $E_{W^\pm}$ are the energies of the individual W bosons.

Next, cuts are applied which require that the $W^+W^- \to W^+W^-$ events have a large $\sqrt{\hat{s}}$ and are produced at a large angle:

$$M_{WW} > 500\ {\rm GeV};\ p_T(W) > 150\ {\rm GeV};\ |\cos\Theta| < 0.8\ . \tag{3}$$

With these cuts applied Barger *et al.* observed that signal–to-background would be optimized if the p_T of the WW or ZZ system were in the range

$$\begin{aligned} 50\ {\rm GeV} &< p_T(WW) < 300\ {\rm GeV} \\ 20\ {\rm GeV} &< p_T(ZZ) < 300\ {\rm GeV}\ . \end{aligned} \tag{4}$$

Finally, with the above minimum $p_T(WW)$, $p_T(ZZ)$ cuts applied, $e^\pm$ tagging becomes effective in removing events of the type $e^+e^- \to e^+e^-W^+W^-$ and $e^+e^- \to e^-\overline{\nu}W^+Z$. The $e^\pm$ tagging cuts are

$$\text{no } e^\pm \text{ with } E_e > 50\ {\rm GeV} \text{ and } |\cos\theta_e| < \cos(0.15{\rm rad})\ . \tag{5}$$

Fig. 4 shows the M_{WW} and M_{ZZ} distributions after all cuts. The 1 TeV Higgs scalar resonance stands out in both the $\nu\overline{\nu}WW$ and $\nu\overline{\nu}ZZ$ final states. The LET signal is larger for the final state $\nu\overline{\nu}ZZ$ than it is for $\nu\overline{\nu}WW$.

Table I: Signal and background for $e^+e^- \to \nu\overline{\nu}W^+W^-$ and $e^+e^-\nu\overline{\nu}ZZ$ at $\sqrt{s} = 1.5$ TeV with 100 fb^{-1} and 80% inital state electron polarization.

Signal (S) or Background (B)	SM $M_H = 1$ TeV	Vector $M_V = 1$ TeV	LET
$S(\nu\overline{\nu}W^+W^-)$	149	41	28
B	129	3.3	129
$S/\sqrt{B}$	13	23	2.5
$S(\nu\overline{\nu}ZZ)$	108	32	41
B	50	50	50
$S/\sqrt{B}$	15	4.6	5.7

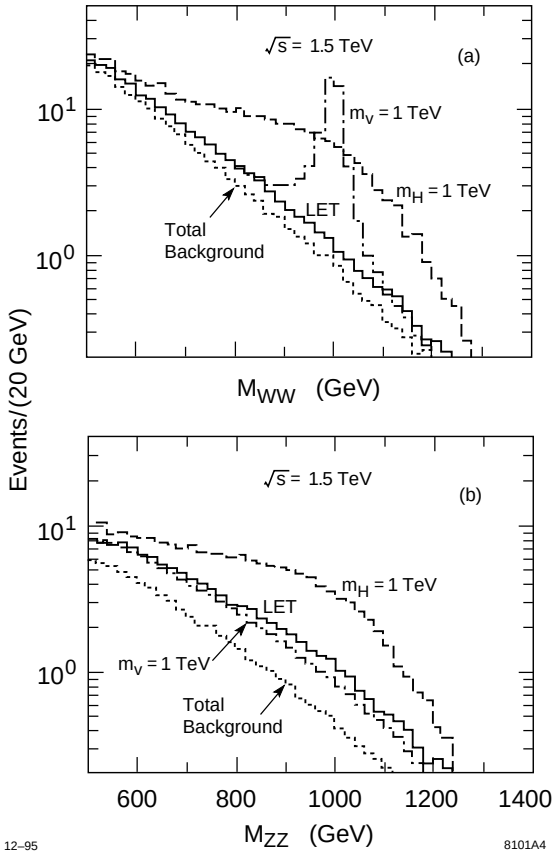

Figure 4: Expected numbers of W^+W^-, $ZZ \to (jj)(jj)$ signal and background events after all cuts for 200 fb^{-1} luminosity at $\sqrt{s} = 1.5$ TeV: (a) $e^+e^- \to \nu\overline{\nu}W^+W^-$, (b) $e^+e^- \to \nu\overline{\nu}ZZ$. Dijet branching fractions and $W^{\pm}/Z$ identification/misidentification factors are included. The dotted histogram shows total SM background including misidentifications. The solid, dashed and dot–dashed histograms show signal plus background for the LET, SM, and CCV models, respectively; CCS model results are close to the SM case.

The statistical significance of the signals for the different models is given in Table I assuming 80% left–handed e^- polarization at $\sqrt{s} = 1.5$ TeV and $100 fb^{-1}$ luminosity. The signal and background counts are the number of events remaining following all of the cuts described above.

Table II: Signal and background for $e^+e^- \to \nu\overline{\nu}W^+W^-$ and $e^+e^-\nu\overline{\nu}ZZ$ at $\sqrt{s} = 1.5$ TeV with 100 fb^{-1}, 90% inital state electron polarization and 65% initial state positron polarization.

Signal (S) or Background (B)	SM $M_H = 1$ TeV	Vector $M_V = 1$ TeV	LET
$S(\nu\overline{\nu}W^+W^-)$	259	72	49
B	202	7.1	202
$S/\sqrt{B}$	18	32	3.4
$S(\nu\overline{\nu}ZZ)$	188	56	71
B	82	82	82
$S/\sqrt{B}$	21	6.2	7.8

It might be possible to increase the electron polarization to 90% and to produce positrons with 65% polarization. The signals and background with these polarizations are given in Table II. The statistical significances are larger by a factor of 1.4, so that this polarization upgrade is equivalent to a factor of two improvement in luminosity. Note that the statistical significance of the LET signal is 7.8σ in the $\nu\overline{\nu}ZZ$ channel.

IV. THE REACTION $e^+e^- \to \nu\overline{\nu}t\overline{t}$

If there is no light Higgs boson then the process $t\overline{t} \to W^+W^-$ violates unitarity at the multi–TeV scale. It is natural then to ask if strong symmetry breaking can be detected through the process $W^+W^- \to t\overline{t}$. This process would be studied at the NLC by observing the reaction $e^+e^- \to \nu\overline{\nu}t\overline{t}$.

The total cross sections [2] for $e^+e^- \to e^+e^-t\overline{t}$ and $e^+e^- \to \nu\overline{\nu}t\overline{t}$, as well as the gauge boson helicity components of these cross sections are displayed in Fig. 5. The cross sections are shown as a function of top quark mass assuming that the e^+e^- center of mass energy is 2 TeV. The cross sections for $\sqrt{s} = 1.5$ TeV are similar.

We have used the work of Barger *et al.* as a guide in developing selection criteria for $e^+e^- \to \nu\overline{\nu}t\overline{t}$. We have also made similar assumptions regarding detector performance. Specifically, we assume that the quantities $M_{t\overline{t}}$, $p_T(t)$, and $p_T(t\overline{t})$ are measured well for $|\cos\Theta_t| < 0.8$ when both top quarks decay hadronically. We do not have an issue analogous to the W/Z misidentification problem since the top and bottom quark masses are so different. Consequently we assume that hadronically decaying top quarks are reconstructed with 100% efficiency for $|\cos\Theta_t| < 0.8$.

We shall also consider events in which one top quark decays hadronically and the other decays semi-leptonically. We must alter our selection criteria for these events since the quantities

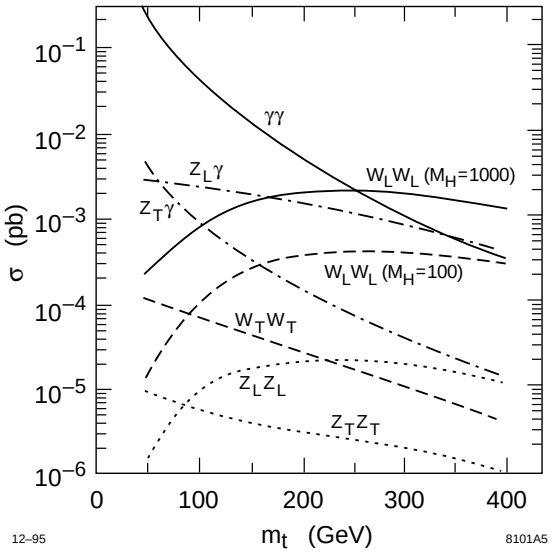

Figure 5: Contributions from various subprocesses to the total cross sections for $e^+e^- \to e^+e^-t\bar{t}$ and $e^+e^- \to \nu\overline{\nu}t\bar{t}$. The contributions are plotted as a function of the top quark mass m_t. The e^+e^- center of mass energy is 2 TeV.

$M_{t\bar{t}}$ and $p_T(t\bar{t})$ cannot be fully reconstructed due to the undetected neutrino produced by the semi-leptonically decaying top.

A. Selection Criteria for $t\bar{t} \to (bjj)(\bar{b}jj)$

Our selection criteria when both top quarks decay hadronically are almost identical to the criteria imposed by Barger *et al.* for $W^+W^- \to W^+W^-$. We require

$$M_{\rm recoil} > 200 \text{ GeV}, \tag{6}$$

$$M_{t\bar{t}} > 500 \text{ GeV}; p_T(t) > 150 \text{ GeV}; |\cos\Theta_t| < 0.8\,, \tag{7}$$

$$30 \text{ GeV} < p_T(t\bar{t}) < 300 \text{ GeV}, \tag{8}$$

and

$$\text{no } e^{\pm} \text{ with } E_e > 50 \text{ GeV and } |\cos\theta_e| < \cos(0.15\text{rad})\,. \tag{9}$$

B. Selection Criteria for $t\bar{t} \to (bl\nu)(\bar{b}jj)$

In this section we consider the event topology $e^+e^- \to \nu_e\overline{\nu}_e t\bar{t} \to \nu_e\overline{\nu}_e(bl\nu_l)(\bar{b}jj)$ where $l = e, \mu$. We would like to reconstruct the momentum three–vector of the neutrino from the top decay (ν_l). These 3 unknowns are one more in number than the two available constraints (one W boson mass and one top quark mass constraint). We deal with this deficit by allowing one of the unknowns to vary over all possible values as we solve for the two remaining unknowns. In this way we obtain a series of solutions for quantites such as $M_{t\bar{t}}$, $p_T(t\bar{t})$ and $\cos\Theta_t$. Cuts are then applied to the maxima and minima of these quantities.

We work in the rest frame of the initial e^+e^- with the z-axis pointing in the direction of the charged lepton l produced by the semi-leptonically decaying top quark. Let $(E_l, \vec{p_l})$, $(E_\nu, \vec{p_\nu})$ and $(E_b, \vec{p_b})$ be the four–vectors for the charged lepton, neutrino, and b quark, respectively, that are produced by the semi-leptonically decaying top quark. Let (θ, ϕ) be the polar and azimuthal angles of the neutrino produced by the semi-leptonically decaying top quark.

If we impose the W boson mass and top mass constraints and assume that the charged lepton is massless, then the neutrino energy E_ν satisfies the equation

$$\mathrm{A}E_\nu^2 + \mathrm{B}E_\nu + \mathrm{C} = 0, \tag{10}$$

where

$$\begin{aligned}
\mathrm{A} &= (E_b - p_{b_z})^2 \\
\mathrm{B} &= \frac{m_W^2}{E_l}\left[E_b p_{b_z} - \left(\psi^2 + p_{b_z}^2\right)\right] + G\left(E_b - p_{b_z}\right) \\
\mathrm{C} &= \frac{1}{4}\left[G^2 + \frac{m_W^2}{E_l}\left[\frac{m_W^2}{E_l}\left(\psi^2 + p_{b_z}^2\right) + 2p_{b_z}G\right]\right] \\
\psi &= p_{b_x}\cos\phi + p_{b_y}\sin\phi \\
G &= m_b^2 + m_W^2 + 2(E_bE_l - p_{b_z}E_l) - m_t^2 \quad .
\end{aligned} \tag{11}$$

We allow ϕ to vary between $0 \le \phi \le 2\pi$ and solve for E_ν. Given E_ν, $\cos\theta$ can be calculated using the W boson mass constraint:

$$\cos\theta = \left(1 - \frac{m_W^2}{2E_\nu E_l}\right) \quad . \tag{12}$$

The two–fold ambiquity in the solution to Eq. (10) can often be resolved by recognizing that all solutions to Eq. (10) satisfy the relation

$$(2\psi E_\nu \sin\theta)^2 = (G + 2E_bE_\nu - 2p_{b_z}E_\nu\cos\theta)^2\,, \tag{13}$$

whereas only solutions of interest satisfy the more restrictive condition

$$2\psi E_\nu \sin\theta = G + 2E_bE_\nu - 2p_{b_z}E_\nu\cos\theta \tag{14}$$

that follows directly from the top mass constraint.

Variables such as $M_{\rm recoil}$ and $p_T(t\bar{t})$ become functions of ϕ when this method is employed. In order to impose selection criteria we define the following variables:

$$\begin{aligned}
\mathcal{M}_{\rm recoil} &= \min_{0\le\phi\le 2\pi} M_{\rm recoil}(\phi) \\
\mathcal{M}_{t\bar{t}} &= \min_{0\le\phi\le 2\pi} M_{t\bar{t}}(\phi) \\
\mathcal{P}_T(t) &= \min_{0\le\phi\le 2\pi} p_T(t)(\phi) \\
\mathcal{P}_T(t\bar{t}) &= \min_{0\le\phi\le 2\pi} p_T(t\bar{t})(\phi) \\
\mathcal{C}_\Theta &= \max_{0\le\phi\le 2\pi} |\cos\Theta_t|(\phi) \quad .
\end{aligned} \tag{15}$$

The following cuts are applied:

$$\mathcal{M}_{\rm recoil} > 10 \text{ GeV}, \tag{16}$$

$$\mathcal{M}_{t\bar{t}} > 450 \text{ GeV};\ \ \mathcal{P}_T(t) > 65 \text{ GeV};\ \ \mathcal{C}_\Theta < 0.9\,, \tag{17}$$

$$15 \text{ GeV} < \mathcal{P}_T(t\bar{t}), \tag{18}$$

$$\text{no } e^{\pm} \text{ with } E_e > 50 \text{ GeV and } |\cos\theta_e| < \cos(0.15\text{rad}) \,. \tag{19}$$

These cut values were chosen so that background processes would have the same detection efficiencies in the $t\bar{t} \to (bl\nu)(\bar{b}jj)$ and $t\bar{t} \to (bjj)(\bar{b}jj)$ topologies. The detection efficiency for signal processes with the $t\bar{t} \to (bl\nu)(\bar{b}jj)$ topology is then 94% of the $t\bar{t} \to (bjj)(\bar{b}jj)$ detection efficiency.

C. Signal and Background

Table III: Signal and background for $e^+e^- \to \nu\overline{\nu}t\bar{t}$ at $\sqrt{s} = 1.5$ TeV with 100 fb^{-1} and 80% inital state electron polarization. The contributions from the event topologies $t\bar{t} \to (bjj)(\bar{b}jj)$ and $t\bar{t} \to (bl\nu)(\bar{b}jj)$ are summed together.

Signal (S) or Background (B)	SM $M_H = 1$ TeV	Vector $M_V = 1$ TeV	LET
$S(\nu\overline{\nu}t\bar{t})$	132	–	53
B	36	–	36
$S/\sqrt{B}$	22	–	8.8

Table IV: Signal and background for $e^+e^- \to \nu\overline{\nu}t\bar{t}$ at $\sqrt{s} = 1.5$ TeV with 100 fb^{-1}, 90% inital state electron polarization and 65% initial state positron polarization. The contributions from the event topologies $t\bar{t} \to (bjj)(\bar{b}jj)$ and $t\bar{t} \to (bl\nu)(\bar{b}jj)$ are summed together.

Signal (S) or Background (B)	SM $M_H = 1$ TeV	Vector $M_V = 1$ TeV	LET
$S(\nu\overline{\nu}t\bar{t})$	229	–	92
B	51	–	51
$S/\sqrt{B}$	32	–	13

The signals and background for $\nu\overline{\nu}t\bar{t}$ are given in Table III assuming 80% e^- polarization and 0% e^+ polarization at $\sqrt{s} = 1.5$ TeV and $100 fb^{-1}$ luminosity. The hadronic and semi-leptonic branching fractions of the top quark are properly accounted for, and the 6% loss in detection efficiency for signals in the $t\bar{t} \to (bl\nu)(\bar{b}jj)$ topology, $l = e, \mu$, relative to the $t\bar{t} \to (bjj)(\bar{b}jj)$ topology is included. We also make the assumption that the $t\bar{t} \to (bl\nu)(\bar{b}jj)$ topology with $l = \tau$ can be utilized with a 50% loss in efficiency relative to $t\bar{t} \to (bjj)(\bar{b}jj)$; we have not demonstrated that this can be accomplished in this paper, but we are confident that future studies of top quark decays to tau leptons will obtain efficiencies at least this good.

The signals and background for 90% e^- polarization and 65% e^+ polarization are shown in Table IV. Just as for $W^+W^- \to W^+W^-$, we see that there is considerable improvement when both the electron and positron beams are polarized.

Table V: Signal and background for $e^+e^- \to \nu\overline{\nu}t\bar{t}$ at $\sqrt{s} = 1.0$ TeV with 100 fb^{-1}, 90% inital state electron polarization and 65% initial state positron polarization. The contributions from the event topologies $t\bar{t} \to (bjj)(\bar{b}jj)$ and $t\bar{t} \to (bl\nu)(\bar{b}jj)$ are summed together.

Signal (S) or Background (B)	SM $M_H = 1$ TeV	Vector $M_V = 1$ TeV	LET
$S(\nu\overline{\nu}t\bar{t})$	26	–	15
B	8.1	–	8.1
$S/\sqrt{B}$	9.2	–	5.1

Even at $\sqrt{s} = 1.0$ TeV there are interesting signals for a $m_H = 1$ TeV standard model Higgs and for the LET model. The statistical significanes of signals for $\sqrt{s} = 1.0$ TeV are shown in Table V assuming $100 fb^{-1}$ luminosity, 90% polarization for the electron beam, and 65% polarization for the positron beam.

D. Final State Helicity Analysis of $\nu\overline{\nu}t\bar{t}$

The strong symmetry breaking signal can perhaps be further enhanced by performing a helicity analysis on the $t\bar{t}$ final state to isolate the helicity combinations $t_L\bar{t}_L$ and $t_R\bar{t}_R$. Recall from Sec. II.A that these were the helicity combinations responsible for the $m_t\sqrt{s}$ growth in the amplitude for $W^+W^- \to t\bar{t}$. Projecting out these helicity combinations would be the analog of projecting out the $W^+_{\rm L}W^-_{\rm L}$ and Z_LZ_L final states in gauge boson scattering.

V. CONCLUSION

The process $e^+e^- \to \nu\overline{\nu}t\bar{t}$ appears to be an effective means to study strong symmetry breaking in the fermion sector. Even in a scenario with no resonances, this process gives good signals at an e^+e^- linear collider with $\sqrt{s} = 1000 - 1500$ GeV. It remains to be seen how well the helicity-flipped final states can be isolated. In addition, a full Monte Carlo study with beamstrahlung and detectors effects included is required to verify the parton level estimates given here.

VI. REFERENCES

[1] V. Barger, K. Cheung, T. Han, and R.J.N. Phillips, *Phys. Rev.* **D52**, 3815 (1995).

[2] R.P. Kauffman, *Phys. Rev.* **D41**, 3343 (1990).